



ORIGINAL RESEARCH ARTICLE

IMPACT OF ACCELERATED CARBONATION CURING (ACC) ON THE
PROPERTIES OF GUINEA CORN HUSK ASH BLENDED CONCRETE

S. O. Odeyemi^{1*}, M. S. Sholagberu¹, R. Abdulwahab¹, A. A. Adedeji²

¹Department of Civil & Environmental Engineering, Kwara State University, Malete, Nigeria.

²Department of Civil Engineering, University of Ilorin, Ilorin, Nigeria

*Corresponding author's email address: samson.odeyemi@kwasu.edu.ng

ARTICLE
INFORMATION

Submitted 20 April, 2022

Revised 11 June, 2022

Accepted 14 June, 2022

Keywords:

Accelerated Carbonated
Curing
Compressive Strength
Concrete
Guinea Corn Husk Ash
Durability

ABSTRACT

There are different methods of curing concrete. These include immersion in water, sprinkling of the concrete samples, curing with sand or sawdust and open-air curing method. However, research on the use of Accelerated Carbonation Curing (ACC) method for curing concrete is very scanty. Therefore, this study concentrates on determining the impact of ACC on the properties of Guinea Corn Husk Ash (GCHA) Blended Concrete. Materials such as Portland Limestone Cement, Guinea Corn Husk Ash (GCHA), sand, and granite dust were tested for fineness, coarseness, specific gravity before they were used for producing the concrete. Characterizations, such as Scanning Electronic Microscopy (SEM), Energy Dispersive X-Ray Fluorescence Spectrometry (EDXRF) and X-Ray Diffraction (XRD) were performed to investigate the properties of the GCHA. The batched concrete was then cured using the ACC and Water Curing (WC) methods. Mix ratios of 0%, 5%, and 10% GCHA were utilized in obtaining the highest compressive strength. Compressive strength for 0%, 5%, 10% incorporation of GCHA in concrete for both ACC and WC methods of curing at 56th day were found to be 23.3 N/mm² and 24.5 N/mm²; 19.1 N/mm² and 21.7 N/mm²; 11.1 N/mm² and 11.8 N/mm² respectively. The highest sorptivity values were obtained at 10% replacement of cement with GCHA for both ACC and WC cured samples. However, the Sorptivity values decreased as the curing age increases both for ACC and WC cured concrete. This demonstrates that both methods produced durable concrete.

© 2022 Faculty of Engineering, University of Maiduguri, Nigeria. All rights reserved.

1.0 Introduction

Since the industrial revolution, global warming has become a big problem for a sustainable future. The upsurge in global warming in the last five (5) decades cannot be overlooked. Carbon (iv) oxide (CO₂) is the main greenhouse gas that leads to global warming. When CO₂ gets accumulated in the air and traps heat, it consequently leads to an increase in temperature on earth. There are many sources of carbon (iv) oxide emissions, however, burning of fossil fuels and the production activities of manufacturing companies are the chief source of global CO₂ emissions. Cement manufacturing industries produce more than 5% of the world's CO₂ emissions (Chen and Zhang, 2010). Studies have shown that about 0.98 tons of CO₂ equivalent are discharged in the production of one ton of cement clinker (Qian et al., 2018). Turner and Collins (2013) estimated that 1.22 kg of CO₂ are discharged into the atmosphere for each kilogram of cement produced. Hence, it is pertinent to utilize the wasted CO₂ in the development of strong and low-cost concrete (Adeyemi and Malachi, 2020). El-Hassan (2020) recommended ACC as a means of reducing CO₂ emissions, thus preserving the world.

Ahmad *et al.* (2017) defined carbonation as a process of diffusion where CO₂ gas in the atmosphere infiltrates concrete and in the presence of water produces carbonic acid. This acid reacts with the Ca(OH)₂ in concrete to form CaCO₃. The CaCO₃ produced owing to the carbonation process makes the resulting concrete dense, thereby improving its properties. Carbonation of cementations materials is accountable for the reduction of pH value which results in the concrete becoming less alkaline. Hence the process of carbonation of concrete is sometimes known as neutralization process.

There are different methods of curing concrete, which includes; immersion in water, sprinkling of the concrete samples, curing with sand and in some cases sawdust, and open-air curing method (Atoyebi *et al.*, 2020; James *et al.*, 2011; Odeyemi *et al.*, 2021). Nevertheless, research implementing ACC for concrete curing is few. For example, Kim *et al.* (2022) considered the effect of carbonation curing on the properties of cement mortar containing appreciable level of belite and exposed to high temperatures. Their findings show that heat resistance of cement mortar relative to that of samples cured in water was enhanced by carbonation curing. Zhang *et al.* (2017) carried out a review on carbonation curing of some cement-based materials. Though some findings were reported, the review recommended further laboratory and industrial research on the subject matter.

In the same vein, research abound on the usage of GCHA as a possible partial replacement for cement in concrete (Aburime *et al.*, 2020; Alkamu *et al.*, 2018; Bello *et al.*, 2018; Ndububa and Yakubu, 2015; Odeyemi, Anifowose, *et al.*, 2020; Odeyemi, Atoyebi, *et al.*, 2020). However, these authors adopted the method of immersion in water to cure their concrete samples but none of them considered the use of ACC. Hence, the current study was designed to determine the impact of ACC method on the properties of GCHA Blended Concrete.

2.0 Materials and Methods

2.1 Materials

2.1.1 Binder

Portland Limestone Cement of Dangote brand [Grade 42.5R], was adopted in this research because it is the mostly used binder in the area of study. Soundness, normal consistency, and fineness test were conducted on the cement before use according to BS EN 12620:2002+A1:2008 (2008).

2.1.2 Water

Potable water, free from deleterious materials, was utilized for mixing the concrete used in this research. It was tested for its pH value using portable pH meter (S-903) housed at the Department of Civil Engineering Water Laboratory, University of Ilorin, Ilorin, Nigeria.

2.1.3 Fine Aggregate

The sharp sand (fine aggregates) adopted for this study was collected from Asa River, in Ilorin. Laboratory tests such as specific gravity and fineness modulus were carried out as stipulated in BS EN 933-1 (2012), water absorption and sieve analysis, were conducted on the sharp sand in accordance with BS ISO 3310-2 (2013).

2.1.4 Coarse Aggregate

Coarse aggregate (crushed stone) which was locally sourced was utilized in this study. The coarse aggregate was sieved to a minimum particle-size distribution ranging from 4.75 to 10 mm. Tests such as specific gravity, Aggregate Crushing Value (ACV), and water absorption were conducted on the aggregate in accordance with the standard specified in BS EN 12620:2002 A1+2008 (2008).

2.1.5 GCHA

The Guinea Corn Husk (GCH) was sourced from farmlands at Alapa and Otte, in Asa Local Government Area of Kwara State. The husk was calcinated at a temperature of 650 °C as recommended by Bello et al. (2018) using a Thermolyne furnace at the Foundry and forging workshop, Department of Mechanical Engineering, Institute of Technology, Kwara State Polytechnic, Ilorin. The resulting ashes from the calcination process were grinded to finer particles using a milling machine before sieving with 75 µm sieve to obtain a uniform size distribution.

2.2 Methods

2.2.1 Fineness Test on Portland Limestone Cement and GCHA

The cement and GCHA used in this study were sieved with No. 9 (90 microns) sieve size to obtain their fineness. An empty pan of a known weight was used to hold one hundred (100) grams of the samples. The weight of the pan with the cement/GCHA was determined and recorded. For a period of 15 minutes, the cement was sieved through circular and vertical motions. The weight of the residue on the sieve was recorded. Equation 1 was used to calculate the fineness of the samples.

$$\text{Fineness} = \frac{\text{Percentage of Sample Retained on Sieve}}{100} \quad (1)$$

2.2.2 Fineness Modulus Test

The fineness modulus was determined following the procedure enumerated in BS EN 933-1 (2012). The fineness modulus of the samples was found with Equation 2 by totaling the percentage of retained aggregates on individual sieves and dividing the outcome by 100. The test sample was dried in an oven at a temperature of 110 ± 5 °C before weighing. Afterwards, the samples were sieved using a set of BS sieves on an electric sieve shaker. After the sieving process, the weight of the samples on each sieve was taken and recorded. The summation of weight of samples on individual sieves was calculated as a ratio of the total sample weighed.

$$\text{Fineness Modulus} = \frac{\text{Total Cumulative \% Retained}}{100} \quad (2)$$

2.2.3 Specific Gravity Test

Specific gravity of the sample was conducted in accordance with BS 1377-3:2018+A1:2021 (2018). The samples were painstakingly checked on BS sieves to get rid of deleterious materials. An empty bottle was weighed, and the weight designated as W_1 . The test sample was inserted into the empty bottle and weighed. The weight of both (i.e., the bottle and sample) was recorded as W_2 . Distilled water was poured into the bottle until it reached a marked point. Entrapped air and water bubbles at the surface water were removed by shaking the bottle vigorously. The weight of the bottle, with sample and distilled water was designated as W_3 . Subsequently, the bottle was emptied and kept in an oven. Upon removal from the

oven, distilled water was introduced into the dry bottle to the gauge mark and recorded as W_4 . Equation 3 was then used to calculate the specific gravity.

$$\text{specific gravity} = \frac{W_2 - W_1}{(W_4 - W_1) - (W_3 - W_2)} \quad (3)$$

2.2.4 Soundness Test

This test was conducted as specified by Neville (2011). In conducting the test, standard consistency of cement was required. 400g of cement was used for this experiment. Paste of cement was well mixed and filled into Le-Chatelier's mould. The upper surface of the paste in the mould was cleaned and smoothed before placing a small weight over the cover lid. Immediately, the mould was inserted in water whose temperature was 27°C and left for 24 hours. Thereafter, the mould was taken out from water and the distance between the indicator point was measured as Reading 1. Afterwards, the mould was placed in boiling water for 3 hours. After the stated time, the mould was taken out of the boiling water and made to cool at room temperature. The gap between the indicator points was also recorded as Reading 2. Equation 4 was adopted in determining the soundness of the cement.

$$\text{Soundness of cement} = (\text{Reading 2}) - (\text{Reading 1}) \quad (4)$$

2.2.5 Normal consistency for cement

The normal consistency of the cement was determined following the procedure specified by Odeyemi et al. (2022). 300g of cement was placed on a mixing plate. A crater was formed at the center in which 75ml of water was added. Within 30 seconds, the material was turned and thoroughly squeezed with hand for at least one minute. Thereafter, it was pasted into a ball and tossed from one hand to the other for about six (6) times while keeping the hands 15 cm apart. Then, with the ball in the hollow of one hand, the material was hard-pressed into the mould through its larger end and smoothen off the top with a trowel. The mould was placed with its bigger end on a glass plate and smoothen off at the smaller end. Thereafter, the mould resting on the glass plate under the plunger was raced in the Vicat apparatus. The scale was then set to zero bringing the end of the plunger in touch with the paste surface and then released. The penetration was noted. The experiment was repeated with trial pastes containing different percentages of water. The volume of water mixed was calculated as a fraction by weight of the dry cement as given by Equation 5.

$$\text{Normal Consistency} = \frac{\text{sum of the plunger's penetration of sample 1 and 2}}{2} \quad (5)$$

Sample 1 = first trial of paste made; Sample 2 = second trial of paste made.

2.2.6 Setting Time Test

After determining the normal consistency of the sample, 1 mm size square needle was inserted to the lower end of a Vicat apparatus and made to get in touch with the top of the paste following the procedure reported in Neville (2011). The scale of the apparatus was set to avoid error due to parallax before releasing the needle and noting the penetration. The experiment was repeated until the paste had sufficiently stiffened to prevent the needle from penetrating no further than 5 - 7mm from the lower end of the mould. The time when this was achieved was recorded as the setting times as shown in Equations 6a and 6b.

$$IST = T_2 - T_1 \quad (6a)$$

$$FST = T_3 - T_1 \quad (6b)$$

Where IST = Initial Setting Time; FST = Final Setting Time; T_1 =Time of first initial setting needle penetration; T_2 =Time of final initial setting needle penetration; T_3 =Time of final initial setting needle penetration.

2.2.7 Water absorption test

The water absorption capacity was determined following the procedure used by Odeyemi et al. (2022). Aggregate of 2 kg was used in this experiment. It was washed and placed in a wire basket. This basket was then submerged in water at 27 °C. The air entrapped in the basket was taken away from the sample by lifting the basket 25 mm from the bottom of the tank and then allowing it to drop 25 times at the rate of one drop per second. Thereafter, the aggregate was kept in water for 24 hours. The basket and aggregate were weighed while kept in water. Subsequently, they were taken out of water and dried with an absorbent cloth before weighing. The aggregate was then heated in an oven for 24 hours at to 100 °C. Upon removal from the oven, the aggregate was cooled in an airtight container before weighing. The water absorption (%) was calculated using Equation 8.

$$\text{Water Absorption (\%)} = \frac{(W_1 - W_2)}{W_2} \times 100 \quad (7)$$

W_1 (g) = Weight of air-dried aggregate; W_2 (g) = Weight of oven dry aggregate

2.2.8 Sieve analysis Test

This sieve analysis test was performed on both the fine and coarse aggregates to determine their particle size distribution as recommended by Odeyemi et al. (2020). The aggregates were oven dried at 105 °C. A set of BS sieves was then used for sieving. For the fine aggregate, the size of the sieve ranged from 0.075 mm to 2.36mm with a receiver placed at the bottom of the sieves. For the coarse aggregate, the size of the sieves ranged from 4.76 mm to 31.75 mm with a receiver also placed at the bottom of the sieves. The sieve was thereafter shaken vigorously. The particles of the aggregate were then collected and weighed respectively and used in the computation of their particle size distribution curve.

2.2.9 Aggregate crushing value

The aggregate crushing value was determined following the procedure in Jethro et al. (2013). Aggregate in a plate was weighed and the weight designated as W . The samples were then divided into 3 layers. The individual layers were given 25 strokes of a tamping rod before weighing. The weight obtained was recorded as W_1 . The topmost part of the aggregate was cautiously leveled, and a plunger was fixed to rest horizontally to the surface of the aggregate. Care was taken to ensure that the plunger does not jam in the cylinder. Thereafter, the aggregate with plunger was inserted into the loading platform of the compression testing machine with a loading capacity of 4 tonnes (T). The aggregate was subjected to the load for 10 minutes. The resulting crushed aggregate was sieved with a 200 mm diameter BS sieve 4.00mm stainless steel mesh and loss of fines was avoided. The portion of the aggregate passing through the 200 mm diameter BS sieve was weighed and recorded as W_2 . The percentage of weight of fines formed to the weight of total sample in each test was calculated using Equation 8.

$$\text{ACV} = \frac{W_2 \times 100}{W_1 - W} \quad (8)$$

W_2 = weight of fraction passing through the appropriate sieve (g); $W_1 - W$ = weight of surface dry sample (g)

2.2.10 Scanning Electronic Microscopy (SEM)

The SEM analysis was done at the Material Science and Engineering Laboratory, Kwara State University, Malete following the procedure adopted by Odeyemi et al. (2022). The ASPEX 3020 model of the equipment was used to investigate the surface morphological structure of GCHA. To test the sample, electrons were fired into the sealed vacuum chamber that holds the sample. The sample was coated in gold using Palzer's sputtering device before introducing it under the microscope. The electron beam was brought to a great precision by an electromagnetic coil. Another coil steered the electron beam from one side to another to scan across the sample. The electrons made contact with the surface of the sample before bouncing off it. A detector then records the scattered electrons and converts it to an image. The SEM displayed the image of the sample at different magnifications of 250, 500, 750 and 1000 on a mode of 16 kV accelerating voltage.

2.2.11 Energy Dispersive X-Ray Fluorescence Spectrometry (EDXRF)

The EDXRF analysis was conducted at the Centre of Excellence, Nanotechnology Advance Material in Akure, Ondo State, Nigeria following the procedure adopted by Odeyemi et al. (2022). The Skyray EDXRF analyser (EDX 3600B) was used to determine both the elemental and oxide compositions of the GCHA. The equipment was designed to operate at the following specifications: analyzable element ranging from $11^{Na(sodium)}$ – $92^{U(uranium)}$; analyzable element content ranges dynamically from ppm- level to nearly 100 percent; test time (60sec- 200 sec with extra 50 sec if vacuum requires); inside dimension of sample chamber of 320mm (diam) x 180 mm (height); maximum voltage of 50kV; dimension of spectrometer 650(W) x 466 (H) x 608 (D) mm. To test the sample, the voltage of the equipment was adjusted to ensure adequate power from the x-ray source. The XRD software package on the computer system connected to the equipment was activated and then initialized using pure silicon standard sample. Thereafter, the non-homogeneous sample (GCHA) was ground to a finer and standardized size before loading into the XRD sample holder. The run parameters such as step size, end angle, start angle, and speed were selected, and the sample was scanned. The equipment analyzed the samples relative to peak formations with the XRD standard reference manual and then the operation ended.

2.2.12 X-Ray Diffraction (XRD) on GCHA

The XRD analysis was done at the Centre of Excellence, Nanotechnology Advance Material, Akure, Ondo State (NASANI) following the procedure adopted by Odeyemi et al. (2022). The equipment, (GBC Diffech XRD-MMA), with a model number of EMMA014 and $CuK\alpha$ radiation of $\lambda=1.54060 \text{ \AA}$ was utilized. The equipment specifications include maximum power of 3.0 kW, voltage ranging from 0 – 60 kV, ampere ranging from 0 – 80mA, long term stability 0.01 % over 8 hrs. of performance, ripple displays at 0.003% rms. To achieve a high-resolution scanning, the powder stage had a tripod mounted to allow very precise height adjustment. A variable radius ranging from 175 mm to 250 mm ($K\alpha_1$ and $K\alpha_2$ peaks completely separated at 80 deg with $CuK\alpha$) was adopted. The scanning speed with full multi-pass averaging 0.0002°/min to 60° /min. The range of $2\theta = 0^\circ$ to 70° with scanning step size of 0.002° was used to determine the chemical phase and the crystalline structure of the GCHA.

2.3 Concrete Mixing proportion

Two concrete mixtures having the same mix proportions (1:2:4) containing Portland Limestone Cement (PLC) with GCHA, fine aggregate and coarse aggregate were considered in this study as shown in Table I. The first combination was prepared with PLC as the cementitious material. In the second mixture the Guinea corn husk ash and Portland

Limestone Cement were combined as cementations material. Both concrete combinations were prepared with a water-to-cementitious material ratio of 0.5 to achieve a slump height of 100 mm (± 20 mm) following the recommendations in Odeyemi et al. (2020). After mixing, each of the concrete was divided into equal parts and then cured using ACC and water immersion curing method.

Table I: Weight of Constituent Materials Per Cubic Meter

Materials	Quantity
Portland cement (kg)	205.71
Guinea corn husk ash (5%)	10.28
Guinea corn husk ash (10%)	20.56
Sharp sand (kg)	411.4
Coarse aggregate (granite) (kg)	822.8
Water to cementations material	0.5

2.4 Set up for ACC

Accelerated Carbonation Curing (ACC) chamber for curing the concrete samples was constructed for this experimental study following the schematic diagram found in Assaggaf et al. (2019). A snapshot of the chamber and the orthographic view is shown in Figure 1. The total length, width and height were 1.0 m X 1.0 m X 1.0 m while the inner length, width and height of the chamber that could contain 90 cubes were 0.9m by 0.9m by 0.9m, respectively. The inner part was built in three layers so that 30 cubes could be arranged in each layer. Galvanized plate of 0.6mm thickness was used for the inner construction to prevent the corrosion of the inner chamber. The outer layer thickness was 0.7mm black plate. 'FEV COL PUR' adhesive material was used as a moisture curing polyurethane adhesive, which serve as Glue that bond both the outer layer and the inner layer plates together. This material is in form of liquid but when sprayed into the plate it became glue like. There were two valves that regulate the inflow and out flow of CO₂, one on top of the cylinder gauge and the other at the outlet of chamber. A door was inserted to gain access into the chamber and to mitigate the loss of CO₂ from the chamber.

Two holes were drilled through the wall of the chamber. The inlet hole was connected to the CO₂ cylinder through a hose. A pressure gauge was also connected to the setup to measure the pressure in the ACC chamber. The second hole serves as the outlet for flushing out the CO₂ from the chamber after curing the concrete samples.



(a)

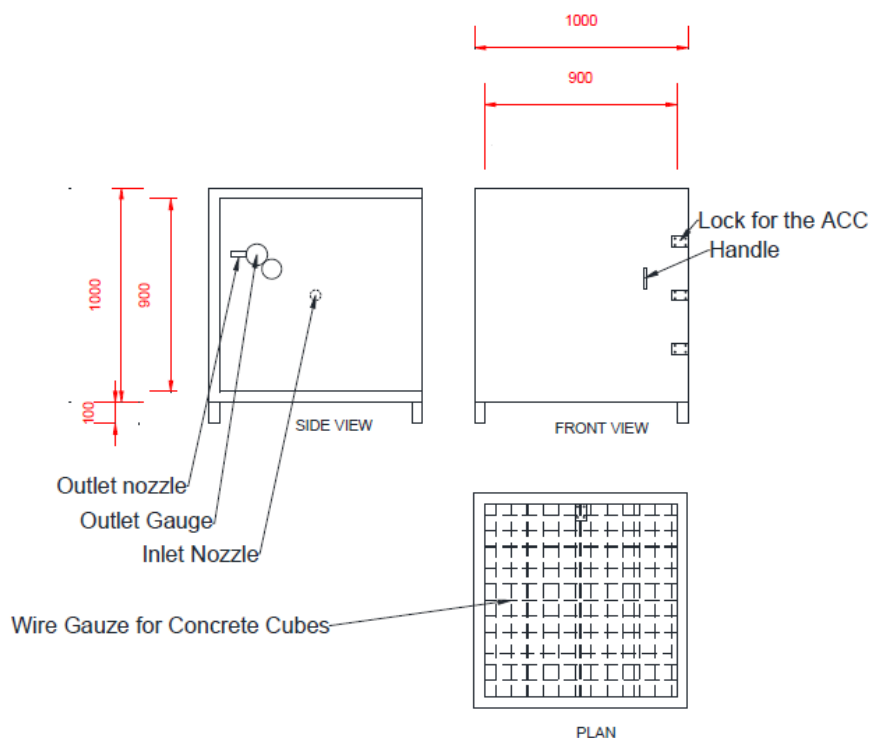


Figure 1: Accelerated Carbonation Chamber (a) Snapshot view (b) Orthographic view

2.5 Curing process

A total of 126 concrete cubes were cast. 18 samples without GCHA were used as control samples and 108 contained varying percentages of GCHA. 63 samples were cured by immersion in water while the remaining 63 were cured in ACC. Thereafter, the chamber was tightly closed to avoid any escape of the gas. CO₂ was allowed to circulate within the chamber for ten (10) hours as was done by Assaggaf et al. (2019). Samples of the cubes were taken out of the chamber after 10 hours to determine their performance in the compression, durability and shrinkage. The samples cured in water were immersed for a maximum number of 56 days before testing.

2.6 Compressive Strength Test

The compressive strength test was carried out following the stipulations in BS EN 12390-3 (2019). The cubes were tested at 7, 28, and 56 days after they were cast. For each method of curing, 3 cubes were crushed at each day of testing to obtain the average strength.

2.7 Durability Test

Two different tests were adopted in determining the durability of the concrete samples as recommended by Fapohunda et al. (2020) viz.: (i) coefficient of water absorption test and (ii) Sorptivity test.

2.7.1 Coefficient of water absorption test

The rate at which the dry concrete samples take up water in one (1) hour was investigated using the method found in Fapohunda et al. (2020). The concrete samples had 100 x 100 x 100 mm dimensions. The specimens were tested after 56 days of curing. The samples were dried in an oven at 105 °C for three (3) days until a stable weight was recorded. Subsequently, the samples were left to cool in an air-tight container for another three (3) days. Since it was

required for water to flow in a direction in this test, all sides except one of the concrete samples were coated with silicone sealant. Then, the samples were partially immersed in a vertical position to a depth of 5 mm at one end, while the remaining sides were exposed to the ambient air. The volume of water absorbed by the concrete samples in the first 60 minutes was determined. Equation 9 was considered in calculating the Coefficient of water absorption (K_a) for the concrete specimens after 56 days curing.

$$K_a = \left[\frac{Q}{A}\right]^2 x \frac{1}{t} \quad (9)$$

Where t =time curing (s), A= Area of concrete (m^2), Q = Quantity of water absorbed (m^3).

2.7.2 Sorptivity test

The tests were carried out at selected times ranging from 0 to 120 minutes as stipulated in Fapohunda et al. (2020). At the times under consideration, the samples were taken from water and excess water dried off using a damp paper towel before weighing the sample. The samples were then placed back in water until another selected time. The gain in mass per unit area over the density of water was plotted versus the square root of the elapsed time. The cumulative water absorption (per unit area of the inflow surface) is thought to increase as the square root of elapsed time (t), increases. The slope of the line of best fit of these points was taken as the sorptivity value. Equation 10 was adopted in determining the sorptivity values of the blended concrete specimens at 7, 28 and 56 days of curing.

$$i = \frac{s}{\sqrt{t}} \quad (10)$$

Where i = sorptivity ($m \cdot s^{-\frac{1}{2}}$); s = slope, t = elapsed time (s)

2.7.3 Shrinkage test on concrete

The shrinkage was determined as specified in Neville (2011). The initial length of the tested specimens L_o (m) was determined and recorded. Afterwards, the length of the sample at each curing age L_t (m) was determined and recorded. The same procedure was adopted for the masses of the samples. The drying shrinkage ratio λ_s (m) and mass loss Δw (g) were calculated using Equations 11a and 11b. The average value of the three specimens tested was recorded as the drying shrinkage value for the sample.

$$\lambda_s = \left(\frac{L_o - L_t}{L_o} \times 100\%\right) \quad (11a)$$

$$\Delta w = (w_o - w_t) \times 100\% \quad (11b)$$

3.0 Results and Discussion

3.1 Test Results for Materials

3.1 Fineness of Cement

Fineness of cement was found to be 1.5%. This result indicates that the cement is very fine and suitable for concrete formation.

3.2 Sieve Analysis Result for Fine Aggregates (Sharp sand)

The Fineness modulus from the sieve analysis was 2.8%. This falls within the range (2.2 % - 3.2%) for fine aggregates. Similar result was obtained by Odeyemi et al. (2020) when they determined the properties of the fine aggregate used in the designing of concrete using GCHA as an additive. Figure 2 confirms the size of the sand particles used in the research as the grain diameter were found to be between 0.080 mm to 2.5 mm with most grains falling in the fine range of particle distribution.

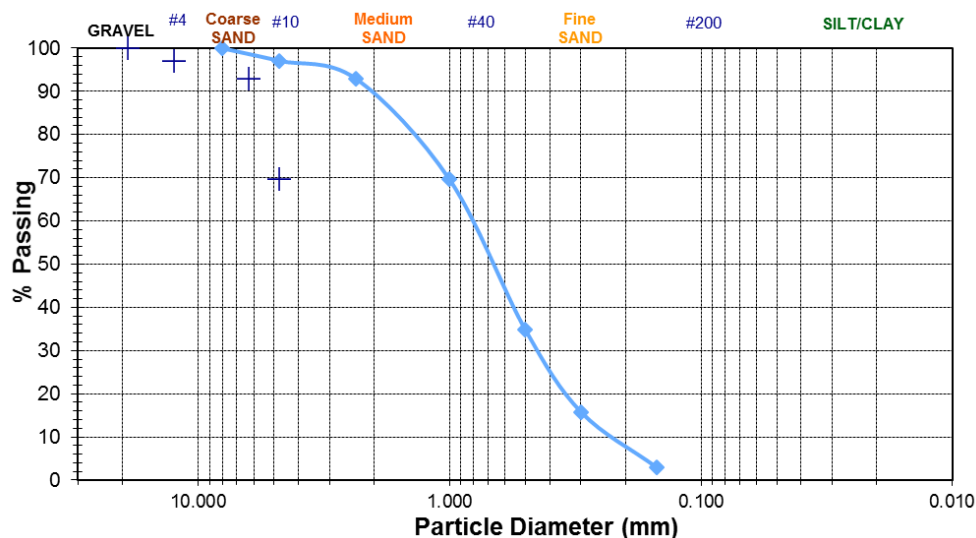


Figure 2: Grain size distribution for fine aggregate

3.3 Sieve Analysis Result for Coarse Aggregate (Granite)

The fine modulus obtained from the sieve analysis was 6.8%. This result falls within the range (5.5%-8.0%) for coarse aggregates. In comparison, the results obtained in this research is quite higher than that obtained by Odeyemi et al. (2020) when they determined the grading of granite used for their concrete. This is because the granite used in this research is coarser than that used in the earlier stated literature. Figure 6 confirms the size of the granite particles used in the research as the grain diameter were found to be between 3.6 mm to 30 mm with most grains falling in the coarse range of particle distribution.

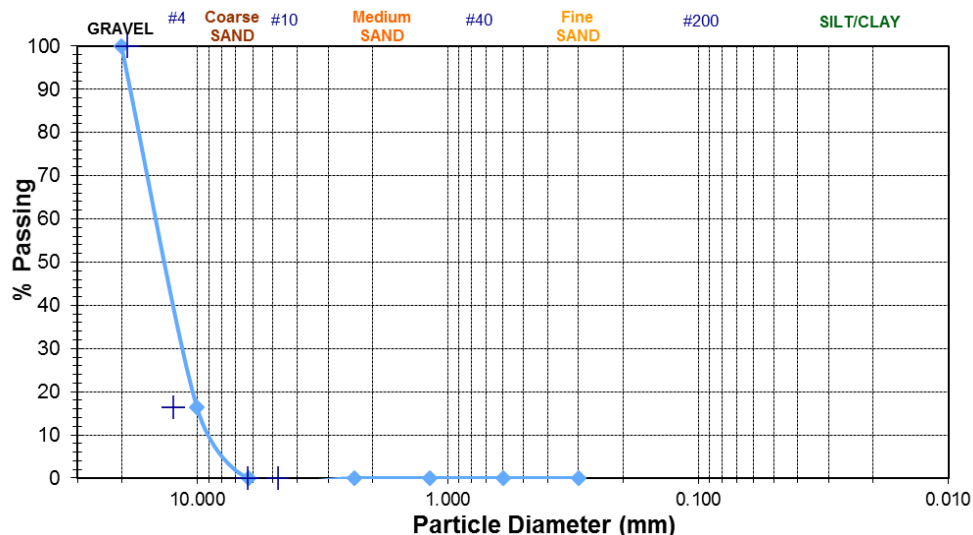


Figure 3: Grain size distribution for Coarse Aggregate

3.4 Specific Gravity (S.G.) of Cement, Sharp Sand and Granite

The S.G. of the cement, sharp sand and granite used in this study was obtained as 3.11, 2.57 and 2.69 respectively. It was observed that the S.G. for cement obtained in this research was similar to that obtained by Tijani et al. (2020) while the specific gravity of coarse aggregate was

the same with that obtained by Odeyemi et al. (2020). Also, the S.G. for the sharp sand fell in the range (2.5-3.0) stated for natural aggregates by Neville (2011).

3.5 Normal Consistency of Portland Limestone Cement

Table 2 shows that the result of the normal consistency of cement was found to be 32% (128ml). When the quantity of water in concrete is lower than the standard consistency, the hydration of cement will be hampered. Also, if the quantity of water is too much there may be reduction in the strength of the cement. Hence, the result suggests that 32% of water (128ml) is required to make a standard consistency cement paste for the research work.

Table 2: Normal Consistency of Cement

Percentage of water by wt. of dry cement (%)	Quantity of water added (ml)	Gauging Time (minutes)	Penetration (mm)
30	120	4	8
31	124	4	30
32	128	4	35
33	132	4	40

3.6 Soundness of cement

The soundness of Portland Limestone Cement used in this research was obtained as 1mm. According to BS EN 196-3:1995 (1995), soundness for ordinary Portland cement must not exceed 10mm. Therefore, since the result obtained was 1mm, the result confirms that the cement can still maintain its shape and volume after it gets hardened.

3.7 Initial and final Setting Time of Cement

The initial setting time was calculated as 1 hour 3 minutes. This indicates the time the cement turns into paste by mixing and begins to lose its plasticity properties. The final setting time was found to be 6 hours and 8 minutes.

3.8 Water Absorption Capacity of Sharp Sand and Granite

The water absorption capacity for sharp sand and Granite were found to be 1.4% and 0.2 % respectively. This indicates that the sharp sand has larger absorption capacity than the granite. It also indicates that the sharp sand has more pores for absorption and could retain more water than the granite.

3.9 Aggregate Crushing Value for granite

The aggregate crushing value was found to be 21.5 %. This indicates that the resistance of the aggregates to failure under an increasing compressive load is high. Jethro et al. (2013) obtained a coarse aggregate value of 21.6 % for granite used in their study and concluded that the resistance of granite is highly durable for engineering work and road construction.

3.10 Quantity of Water

The pH of the water used in this study was found to be 7.5. This indicates a neutral pH. If the water was too acidic or basic, it may attack the concrete by dissolving both hydrated and unhydrated cement compounds or even react with the compounds present in the carbonated guinea corn husk ash, thereby causing shrinkage in the concrete.

3.11 XRD Analysis of Calcined GCHA

Figure 4 illustrates the X-ray diffraction form of the calcined GCHA. It confirmed the presence of a crystalline compound in the calcined GCHA. The peaks at 2 theta (2θ) angles 20.2008° , 28.2348° , 41.0028° , 43.564° , 54.6025° , and 61.9344° are attributed to the presence of SiO_2 (Quartz) particles. The GCHA molecules tend to form a hexagonal crystalline structure. This result is in agreement with what Nandanwar *et al.*, (2015) obtained when they carried out the XRD characterization of SiO_2 particles and obtained an hexagonal shape.

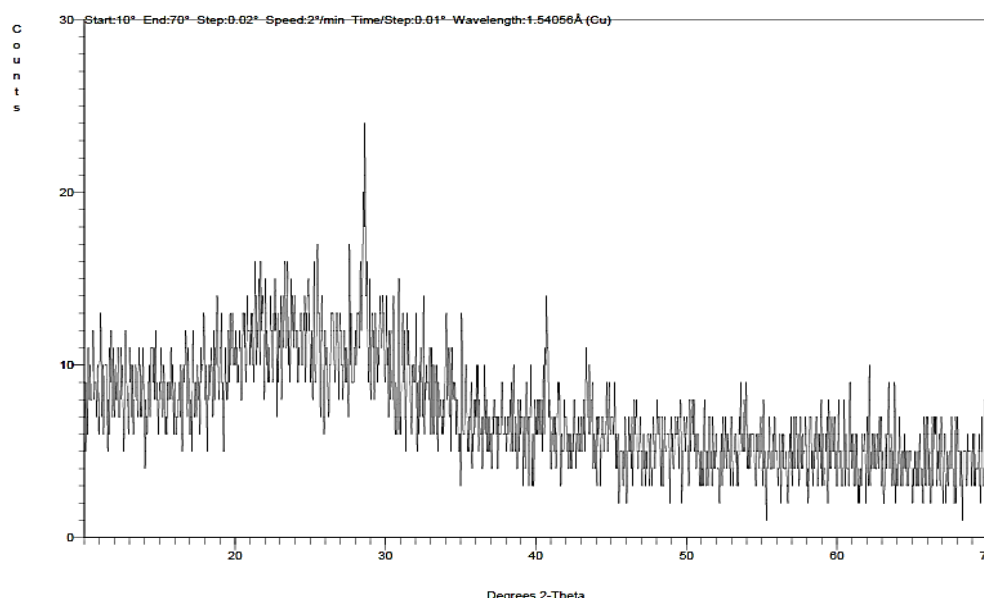


Figure 4: The XRD pattern of the calcined GCHA

3.12 XRF Analysis of Calcined GCHA

Table 3 shows the oxide composition of GCHA. It consists mainly of SiO_2 (63.1559%), K_2O (23.4164%), Al_2O_3 (4.1534%), and Fe_2O_3 (4.6572%). It was discovered that the sum of Al_2O_3 , SiO_2 , and Fe_2O_3 gave 71.9665%. This is above the minimum 70% specified for supplementary cementitious materials by ASTM C618 (Standard Specification for Coal Fly Ash and Raw or Calcined Natural Pozzolan for Use in Concrete, ASTM International, West Conshohocken, PA, 2019, 2019). Odeyemi *et al.* (2020) and Ndububa *et al.* (2015) also obtained similar results. The findings are also in tandem with what was obtained by Odeyemi *et al.* (2022) for bamboo leaf ash (BLA). These further confirms that GCHA is suitable as a pozzolan in concrete.

Table 3: The Oxide composition of Calcined GCHA

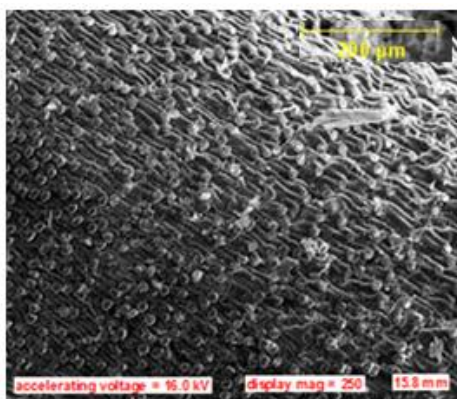
Oxide	Composition (%)
MgO	3.3649
Al_2O_3	4.1534
SiO_2	63.1559
P_2O_5	2.2621
SO_3	4.0899
K_2O	23.4164
CaO	6.9492
TiO_2	0.0000
V_2O_5	0.0000
Cr_2O_3	0.0000
MnO	0.0187

CoO	0.0000
Fe ₂ O ₃	4.6572
NiO	0.0098
CuO	0.0483
ZnO	0.2338
As ₂ O ₃	0.0049
PbO ₂	0.0559
WO ₃	0.3297
Au ₂ O	0.0000
Ag ₂ O	0.0018
Rb ₂ O	0.0489
Nb ₂ O ₅	0.0062
MoO ₃	0.3045
CdO	0.000
SnO ₂	0.4802
Sb ₂ O ₃	0.4169
*LOI	0.0000

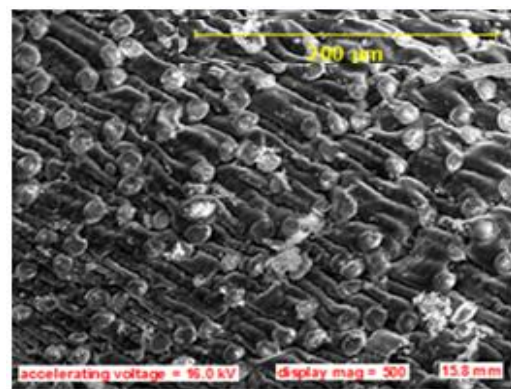
* Loss of Ignition

3.13 SEM Analysis of Calcined GCHA

The morphological structure of the calcined GCHA at 650 °C is revealed in Figure 5. Figure 5(a-d) are of equivalent width of 15.8 mm at 250-1000 magnification. Figure 5(a) shows the image of the GCHA at magnification of 250. The structure contains numerous pores of irregular size. A nearer view of the structure in Figure 5(b) shows that the GCHA at magnification 500 also contains flat-like materials with coarse edges. Moreover, at Figure 4 (c-d), magnifications 750 and 1000 respectively, it was clearly observed that there are discontinuous patterns of arrangement on the GCHA image that are well compact. Therefore, it was inferred that the GCHA calcined at 650°C is a potential material for the substitution of cement in concrete.



(a)



(b)

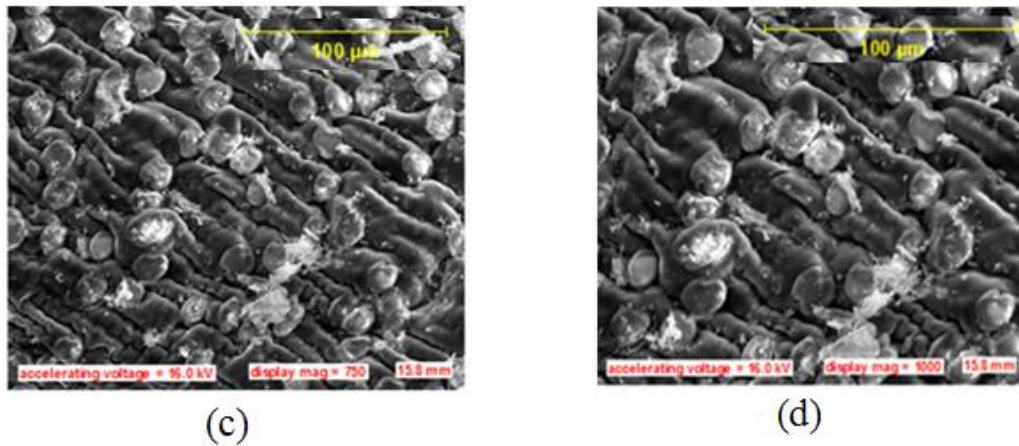


Figure 5: SEM images of calcined GCHA at different magnifications (a) magnification at 250 (b) magnification at 500 (c) magnification at 750 (d) magnification at 1000

3.14 Compressive strength of concrete

The average compressive strengths for 0%, 5% and 10% GCHA inclusion in concrete after being cured by ACC and water curing are revealed in Figure 6. The tests were conducted on the 7th, 28th and 56th day of curing. For the control experiment for ACC, the compressive strength increased from 16.2 N/mm² at day 7 to 23.3 N/mm² at day 56. For the WC, the compressive strength increased from 17.6 N/mm² at day 7 to 24.5 N/mm² at day 56. For 5% inclusion of GCHA in concrete, the compressive strength increased from 12.6 N/mm² at day 7 to 19.1 N/mm² at day 56 and from 13.7 N/mm² at day 7 to 21.7 N/mm² at day 56 for ACC and WC respectively. For 10% inclusion of GCHA in concrete, the compressive strength increased from 6.2 N/mm² at day 7 to 11.1 N/mm² at day 56 and from 7.9 N/mm² at day 7 to 11.8 N/mm² at day 56 for ACC and WC respectively. Hence, from the graph it could be observed that as the ratio of GCHA increases the compressive strength reduced for both ACC and WC concrete. These findings are like those published by Poongodi *et al.*, (2021). Moreover, the ACC method of curing produced results that are close to the results obtained using WC. This follows the same trend of results reported by Assaggaf *et al.* (2019). Furthermore, the advantage in using ACC is that the curing was carried out for only ten (10) hours unlike the immersion method which was done for 56 days.

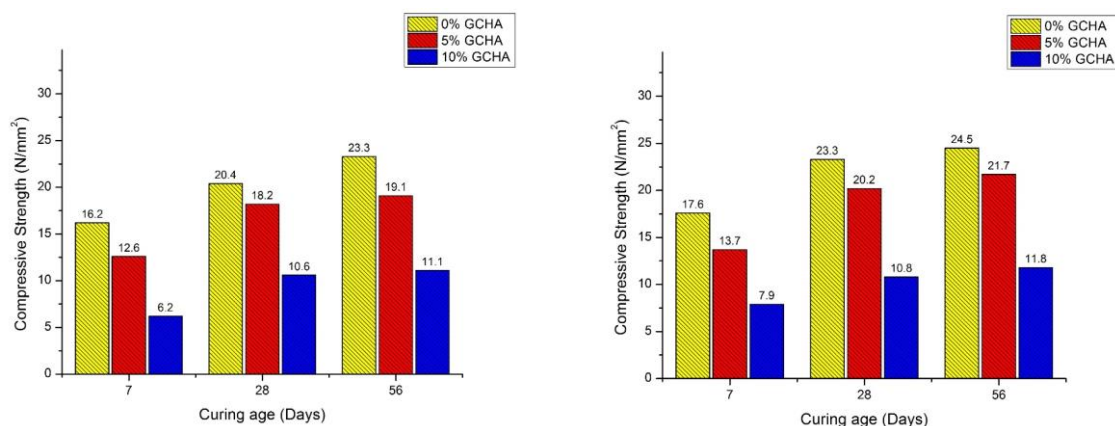
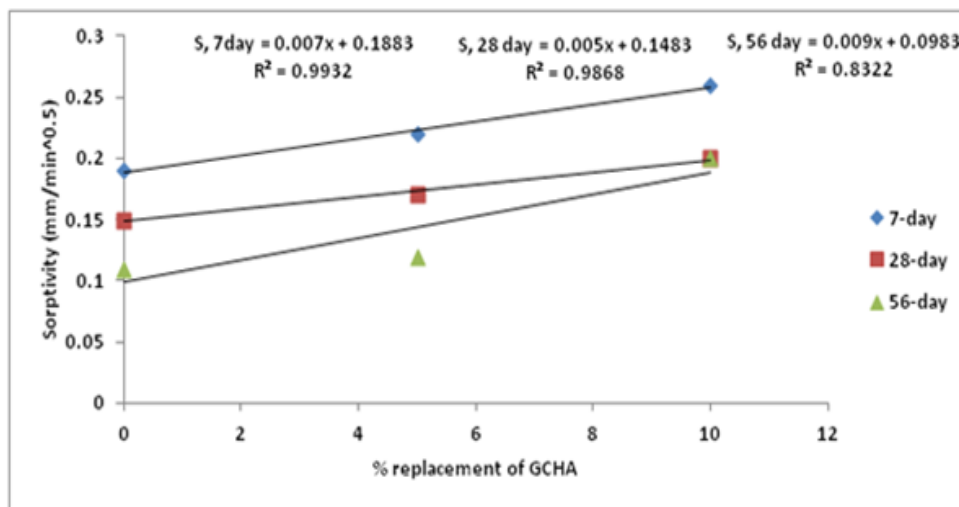


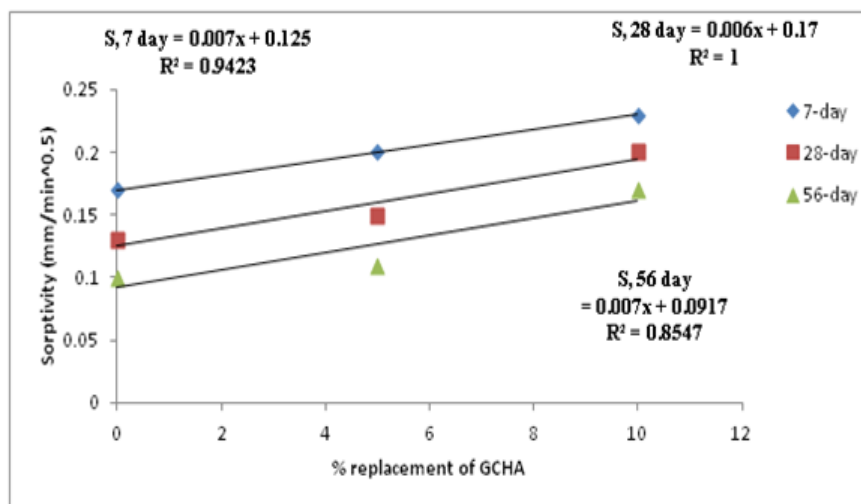
Figure 6: Compressive strength for concrete samples (a) ACC (b) WC (a) 0% GCHA (b) 5% GCHA and (c) 10 % GCHA

3.15 Sorptive behaviour

Figure 7(a) shows the plot of sorptivity against the percentage replacement of GCHA for ACC with R-square values of 0.9932, 0.9868, and 0.8322 at 7, 28 and 56 days of curing respectively. The highest value ($0.26 \text{ mm}/\text{min}^{0.5}$) and lowest value ($0.09 \text{ mm}/\text{min}^{0.5}$) value of sorptivity was obtained at the 7th and 56th day for 10 % GCHA and 0% GCHA respectively. Figure 7(b) shows the plot of sorptivity against the percentage replacement of GCHA for WC with R-square values of 0.9423, 1.0000, and 0.8547 at 7, 28 and 56 days of curing respectively. The highest value ($0.23 \text{ mm}/\text{min}^{0.5}$) and lowest ($0.08 \text{ mm}/\text{min}^{0.5}$) value of sorptivity was obtained at the 7th and 56th day at 10 % GCHA and 0% GCHA for WC respectively. The graph shows the same trends for both ACC and WC. The values of sorptivity are less than $0.1 \text{ mm}/\text{min}^{0.5}$ at 56 days indicating that both curing methods are suitable for concrete development. Similar result was obtained by Cantero et al. (2021) in a study that involves the use of a recycled concrete. This further validates that ACC cured concrete are durable.



(a)



(b)

Figure 7: Sorptivity for Concrete (a) ACC (b) WC

3.16 Water Absorption

Figure 8(a) expresses the plot of water absorption against the percentage replacement of GCHA for ACC. The highest value for the water absorption ($2.91 \text{ m}/\text{s}^2$) was obtained for

10% inclusion of GCHA at 56th day of curing. The graph also reveals that as the level of substituting cement with GCHA increases the water absorption also increases. This indicates that the total reachable pore volume of the concrete becomes more exposed as the percentage GCHA increases. In the same vein, as the number of curing days increases the water absorption also increases. Figure 8(b) shows the plot of water absorption against the percentage replacement of GCHA for WC. The highest value for the water absorption (2.87 %) was obtained for 0% inclusion of GCHA at 56th day of curing. Unlike the ACC method, the 56th day water absorption result decreased with the surge in the proportion of GCHA in the concrete. The results show that the highest value of water absorption occurred in ACC method. This high value in water absorption implies that the ACC method may not be suitable for concrete members kept in water.

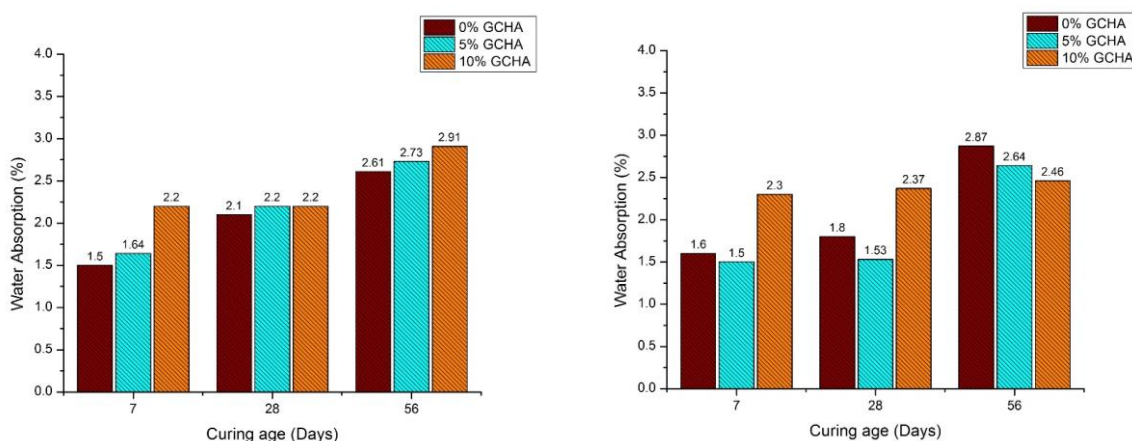


Figure 8: Water Absorption (a) ACC (b) WC

3.17 Shrinkage

Figure 9(a) reveals the change in shrinkage against the percentage replacement of GCHA for ACC. The highest value of shrinkage ($-153 \mu\text{m}/\text{m}$) was obtained after 56 days of curing at 10% inclusion of GCHA. The correlation coefficient at day 7, 28 and 56 were all greater than 0.9. These findings agree with the result of Cantero *et al.* (2021). A similar trend was observed in Figure 9(b) samples cured in WC. The highest value was obtained as $-176 \mu\text{m}/\text{m}$ at day 56 for 10% inclusion of GCHA. The correlation coefficient at day 7 and 28 were greater than 0.9. However, that of 56 days decreased slightly. Hence, in both ACC and WC, the variation in loss of moisture content in the concrete due to hydration of cement and temperature between day 7 and 28 is not as significant when compared to the shrinkage that occurred between day 28 and 56. Generally, the shrinkage tends to reduce as the days of curing increases and as the percentage of GCHA increases.

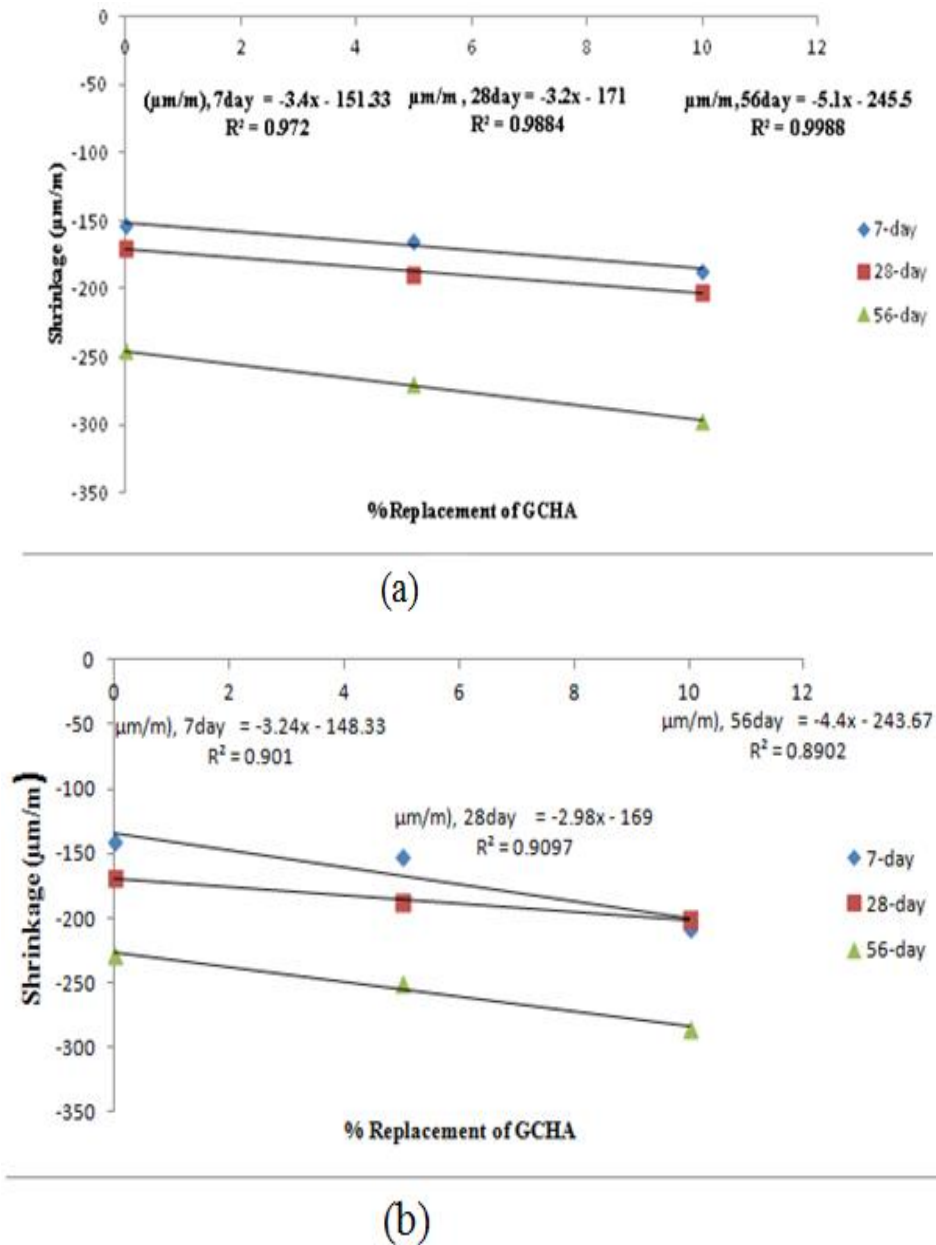


Figure 9: Shrinkage (a) ACC (b) WC

Conclusion

This research studied the impact of ACC on the performance of Guinea Corn Husk Ash Blended Concrete and the following conclusions were drawn.

- The chemical composition of Portland Limestone Cement utilized in the research is within the acceptable range recommended by BS EN 12620:2002+AI (2008) and Guinea Corn Husk Ash (GCHA) satisfies the requirement for a pozzolan and can be adopted as supplementary cementitious material for concrete production.
- The method of curing by immersion in water produced the concrete with the highest strength with a strength value of 21.7 N/mm². This was closely followed by the concrete cured in ACC with a strength value of 19.1 N/mm².
- Both ACC and water immersion curing methods produced concrete that are durable.

Notation

ACC – Accelerated Carbonation Curing
GCHA - Guinea Corn Husk Ash
GCH - Guinea Corn Husk
WC – Water Curing
SEM - Scanning Electronic Microscopy
EDXRF - Energy Dispersive X-Ray Fluorescence Spectrometer
XRD - X-Ray Diffraction

References

- Aburime, Pl., Ndububa, EE. and Kpue, DO. 2020. The Impact of Guinea Corn Husk Ash as an Admixture for Crack Control in Concrete. *European Journal of Engineering Research and Science*, 5(10): 1152–1159. <https://doi.org/10.24018/ejers.2020.5.10.2171>
- Adeyemi, SA. and Malachi, J. 2020. Assessment of the ternary coarse aggregates for economic production of sustainable and low-cost concrete. *Journal of Materials and Engineering Structures*, 7: 25–34.
- Ahmad, S., Assaggaf, RA., Maslehuddin, M., Al-amoudi, OSB., Adekunle, SK. and Ali, SI. 2017. Effects of carbonation pressure and duration on strength evolution of concrete subjected to accelerated carbonation curing. *Construction and Building Materials*, 136: 565–573.
<https://doi.org/https://doi.org/10.1016/j.conbuildmat.2017.01.069>
- Alkamu, T., Emmanuel, I., Datok, EP. and Jambol, DD. 2018. Guinea Corn Husk Ash As Partial Replacement of Cement in Hollow Sandcrete Block Production. *International Journal of Modern Trends in Engineering and Research*, 5(6): 13–19. <https://doi.org/10.21884/ijmter.2018.5163.xllyk>
- Assaggaf, RA., Adekunle, SK., Ahmad, S., Maslehuddin, M., Al-Amoudi, OSB. and Ali, SI. 2019. Mechanical properties, durability characteristics and shrinkage of plain cement and fly ash concretes subjected to accelerated carbonation curing. *Journal of the South African Institution of Civil Engineering*, 61(4): 73–81. <https://doi.org/10.17159/2309-8775/2019/v61n4a7>
- Atoyebi, OD., Ikubanni, P., Adesina, A. and Araoye, OV. 2020. Effect of curing methods on the strength of interlocking paving blocks. *Cogent Engineering*, 7: 1–11. <https://doi.org/10.1080/23311916.2020.1770914>
- Bello, MO., Abdus-Salam, N. and Adekola, FA. 2018. Utilization of Guinea corn (*Sorghum vulgare*) Husk for Preparation of Bio-based Silica and its Characterization Studies. *International Journal of Environment, Agriculture and Biotechnology*, 3(2): 670–675. <https://doi.org/10.22161/ijeab/3.2.48>
- BS 1377-3:2018+A1:2021. 2018. Methods of test for soils for civil engineering purposes - Chemical and electro-chemical testing, BSI Group Headquarters 389 Chiswick High Road, London, W4 4AL, UK, 1-108.
- BS EN 12390-3. 2019. Testing hardened concrete. Compressive strength of test specimens, BSI Group Headquarters 389 Chiswick High Road, London, W4 4AL, UK, 1-24.
- BS EN 12620:2002+A1:2008. 2008. Specification for Aggregates from natural sources for concrete. British Standards, BSI Group Headquarters 389 Chiswick High Road, London, W4 4AL, UK, Standards Policy and Strategy Committee, 1-60.

BS EN 196-3:1995. Methods of Testing Cement-Determination of Setting Time and Soundness, British Standards, BSI Group Headquarters 389 Chiswick High Road, London, W4 4AL, UK, 1-29.

BS EN 933-1. 2012. Tests for Geometrical Properties of Aggregates - Part 1: Determination of Particle Size Distribution - Sieving Method, BSI Group Headquarters 389 Chiswick High Road, London, W4 4AL, UK, 1-22.

BS ISO 3310-2. 2013. Test sieves. Technical requirements and testing - Test sieves of perforated metal plate, BSI Group Headquarters 389 Chiswick High Road, London, W4 4AL, UK, 1-18.

Cantero, B., Bravo, M., Brito de, J., Saez del Bosque, IF. and Medina, C. 2021. Water transport and shrinkage in concrete made with recycled concrete-added cement and mixed recycled aggregate. Cement and Concrete Composites, 118: 103957. <https://doi.org/10.1016/j.cemconcomp.2021.103957>

Chen, GQ. and Zhang, BO. 2010. Greenhouse gas emissions in China 2007: Inventory and input-output analysis. Energy Policy, 38(10): 6180–6193.

El-Hassan, H. 2020. Cement Industry - Optimization, Characterization and Sustainable Application (H. Saleh (ed.)). London, IntechOpen. <https://doi.org/10.5772/intechopen.87890>

Fapohunda, C., Bello, H., Salako, T. and Tijani, S. 2020. Strength, Micro-Structure and Durability Investigations of Lateritic Concrete with Palm Kernel Shell (PKS) as Partial Replacement of Coarse Aggregates. Engineering Review, 40(2): 59–69.

James, T., Malachi, A., Gadzama, EW. and Anametemiok, V. 2011. Effect of Curing Methods on the Compressive Strength of Concrete. Nigerian Journal of Technology, 30(3): 14–20.

Jethro, MA., Shehu, SA. and Olaleye, BM. 2013. The Suitability of Some Selected Granite Deposits for Aggregate Stone Production in Road Construction. The International Journal Of Engineering And Science (IJES), 3(2): 75–81.

Kim, H., Siddique, S. and Jang, JG. 2022. Effect of carbonation curing on the mechanical properties of belite-rich cement mortar exposed to elevated temperatures. Journal of Building Engineering, 52(15): 104453. <https://doi.org/https://doi.org/10.1016/j.jobbe.2022.104453>.

Nandanwar, R., Singh, P. and Fozia, ZH. 2015. Synthesis and characterization of SiO₂ Nanoparticles by Sol-Gel Process and its Degradation. American Chemical Science Journal, 5(1): 1–10.

Ndububa, E. and Yakubu, N. 2015. Effect of Guinea Corn Husk Ash as Partial Replacement for Cement in Concrete. IOSR Journal of Mechanical and Civil Engineering, 12(2): 40–45. <https://doi.org/10.9790/1684-12214045>

Neville, AM. 2011. Properties of Concrete (5th ed.). Pearson Education Ltd., Harlow, Essex, United Kingdom.

Odeyemi, SO., Adisa, MO., Atoyebi, OD., Wilson, UN., and Odeyemi, OT. 2022. Optimal water-cement ratio and volume of superplasticizers for blended cement-bamboo leaf ash high-performance concrete. Research on Engineering Structures and Materials, 8(3): 569-581. <http://dx.doi.org/10.17515/resm2022.382ma0108>

Odeyemi, SO., Abdulwahab, R., Anifowose, MA. and Atoyebi, OD. 2021. Effect of Curing Methods on the Compressive Strengths of Palm Kernel Shell Concrete. Civil Engineering and

Architecture, 9(7): 2286–2291. <https://doi.org/10.13189/cea.2021.090716>

Odeyemi, SO., Anifowose, MA., Abdulwahab, R. and Oduoye, WO. 2020. Mechanical Properties of High-Performance Concrete with Guinea Corn Husk Ash as Additive. LAUTECH Journal of Civil and Environmental Studies, 5: 139–154. [https://doi.org/10.36108/laujoces/0202/50\(0131\)](https://doi.org/10.36108/laujoces/0202/50(0131))

Odeyemi, SO., Atoyebi, OD. and Ayo, E. 2020. Effect of Guinea Corn Husk Ash on the Mechanical Properties of Lateritic Concrete Effect of Guinea Corn Husk Ash on the Mechanical Properties of Lateritic Concrete. IOP Conference Series: Earth and Environmental Science, 1-11. <https://doi.org/10.1088/1755-1315/445/1/012034>

Odeyemi, SO., Atoyebi, OD., Kegbeyale, OS., Anifowose, MA., Odeyemi, OT., Adeniyi, AG. and Orisadare, OA. 2022. Mechanical properties and microstructure of High-Performance Concrete with bamboo leaf ash as additive. Cleaner Engineering and Technology, 6: 1–6. <https://doi.org/10.1016/j.clet.2021.100352>

Poongodi, K., Murthi, P., Awoyera, PO., Gobinath, R. and Olalusi, OB. 2021. Durability Properties of Self-compacting Concrete Made With Recycled Aggregate. Silicon, 1: 2727–2735.

Qian, X., Wang, J., Fang, Y. and Wang, L. 2018. Carbon dioxide as an admixture for better performance of OPC-based concrete. Journal of CO₂ Utilization, 25: 31–38. <https://doi.org/10.1016/j.jcou.2018.03.007>

Standard Specification for Coal Fly Ash and Raw or Calcined Natural Pozzolan for Use in Concrete, ASTM International, West Conshohocken, PA. 2019. <https://doi.org/10.1520/C0618-19>

Tijani, MA., Ajagbe, WC., Ganiyu, AA., Aremu, AS. and Ojewole, YN. 2020. Strength and Absorption of Sorghum Husk Ash Sandcrete Blocks. Premier Journal of Engineering and Applied Science, 1(1): 1–7.

Turner, LK.. and Collins, FG. 2013. Carbon dioxide equivalent (CO₂-e) emissions: A comparison between geopolymer and OPC cement concrete. Construction and Building Materials, 43: 125–130. <https://doi.org/https://doi.org/10.1016/j.conbuildmat.2013.01.023>

Zhang, D., Ghoulah, Z. and Shao, Y. 2017. Review on carbonation curing of cement-based materials. Journal of CO₂ Utilization, 21: 119–131. <https://doi.org/https://doi.org/10.1016/j.jcou.2017.07.003>